



# Simulation of Support Effects in Geotechnical Engineering: A Comparative Study of Concrete and Steel Pipe Piles under Pile-Soil Interaction



Chang Tong<sup>1\*</sup>, Doha Mothefer Al-Saffar<sup>2</sup>

<sup>1</sup> School of Civil Engineering, Qingdao University of Technology, 266520 Qingdao, China

<sup>2</sup> Civil Engineering Department, University of Technology, 10066 Baghdad, Iraq

\* Correspondence: Chang Tong (1416540804@qq.com)

Received: 02-10-2024

Revised: 03-06-2024

Accepted: 03-15-2024

**Citation:** C. Tong, D. M. Al-Saffar, "Simulation of support effects in geotechnical engineering: A comparative study of concrete and steel pipe piles under pile-soil interaction," *GeoStruct. Innov.*, vol. 2, no. 1, pp. 42–52, 2024. <https://doi.org/10.56578/gsi020105>.



© 2024 by the author(s). Published by Acadlore Publishing Services Limited, Hong Kong. This article is available for free download and can be reused and cited, provided that the original published version is credited, under the CC BY 4.0 license.

**Abstract:** In this study, the FLAC3D finite difference numerical software was employed to simulate a geotechnical engineering project, establishing scenarios with concrete and steel pipe piles for support simulation. The analysis focused on the reinforcement effects provided by different types of piles on the geotechnical project. It was found that the reinforcement effects on the soil varied significantly between the pile types. Under the support condition of concrete piles, the maximum soil settlement observed was 4.12 mm, with a differential settlement of 3.19 mm. For steel pipe piles, the maximum soil settlement was reduced to 2.38 mm, with a differential settlement of 2.19 mm, indicating a superior support effect compared to that of concrete piles. Stress concentration phenomena were observed in the piles, becoming more pronounced when pile-soil friction was considered. The substitution of concrete piles with steel pipe piles led to an intensified stress concentration phenomenon in the soil surrounding the piles. The soil undergoing support from concrete piles exhibited the largest plastic deformation, whereas soil supported by steel pipe piles showed less plastic deformation. Consequently, it is concluded that steel pipe piles provide a superior support effect over concrete piles in terms of geotechnical engineering reinforcement.

**Keywords:** Concrete piles; Steel pipe piles; Geotechnical engineering; Numerical simulation; Pile-soil interaction

## 1 Introduction

The bearing capacity and deformation of foundations are central issues in construction engineering, directly impacting the safety of engineering projects. The complex interaction between piles and the surrounding soil, known as pile-soil interaction, involves the mechanical relationship between the pile bodies and the surrounding soil. It is imperative to elucidate the mechanisms through which different types of pile groups affect the foundation, to serve the needs of engineering construction [1–3].

Research on pile-soil interaction has always been a focal point in geotechnical engineering. Liu and Chi [1] proposed a calculation correction model that takes into account the interactions among soil-soil, pile-soil, and pile-pile. Guo et al. [2] studied the patterns of change in horizontal displacement, deformation, and pile body bending moment under cyclic loads. Hu [3] conducted in-situ experiments to investigate the characteristics of soft soil-pile foundation interaction, elucidating the mechanism of interaction induced by road embankment construction on soft soil-pile foundations. Kong et al. [4] analyzed the negative skin friction characteristics of pile groups in clay layers under ground loading conditions, presenting the variation in downdrag forces caused by pile side negative skin friction. Qiu et al. [5] clarified the basic components of pile group settlement based on vertical load settlement characteristic experiments. Mao et al. [6] established a functional relationship between single pile head displacement and equivalent elastic modulus, applying it to calculate the interaction and settlement of pile groups.

Zheng et al. [7] developed a vertical coupled vibration response calculation model for pile-soil-pile interaction, considering the passive pile scattering effect, and provided an analytical solution for the vertical dynamic response of pile groups. Zhang et al. [8] discovered that the non-embedded length of piles, the isotropic parameters of soil, and the liquid-solid coupling coefficient significantly influence the dynamic impedance of pile groups. Ding et al. [9] simulated the horizontal vibration of tubular piles in saturated soil layers using Biot's poroelastic theory,

revealing the impact of second-order effects of axial loads on the horizontal dynamic response of tubular piles. Ai et al. [10] employed the analytical layer element method to simulate the dynamic response of pile groups, elucidating the effects of embedding ratio, pile spacing, and pile-soil modulus ratio on dynamic impedance. Zhang et al. [11] analyzed the impact of pile non-embedded length and soil's isotropic parameters on the vibration characteristics of pile groups. Luan et al. [12] considered the secondary waves generated by the vibration of receiver piles, introducing a dynamic coupling factor to modify the pile-to-pile interaction factor. Sheil et al. [13] analyzed the importance of addressing soil stiffness nonlinearity and evaluated the applicability of various simplified models. Zhou et al. [14] investigated the application of a new type of XCC pile in soil displacement, proposing a modified model to better predict its displacements induced during construction. Zheng et al. [15] developed an analytical solution to study the vertical vibration of pipe piles in viscoelastic soil, revealing their dynamic characteristics. Anoyatis et al. [16] revisited the dynamic soil reaction of laterally-loaded piles, proposing an analytical model to more accurately describe soil behavior. Torshizi et al. [17] investigated the dynamic response of end-bearing fixed-head cylindrical pile groups under harmonic shear waves and its influencing factors. Ai et al. [18] studied the behavior of pile groups in multilayered soils using finite element and analytical methods, exploring the effects of various factors. Cui et al. [19] explored the dynamic impedance of pipe piles in layered soils, proposing an analytical approach to predict their response. Padrón et al. [20] presented a BEM-FEM coupling model for analyzing the time harmonic dynamic behavior of piles and pile groups in elastic half-space.

Concrete and steel pipe piles are widely used in foundation pit support engineering, yet the difference in support effects under various geological conditions remains unclear, lacking a comparative analysis of the support effects of different types of piles. Certain equipment, being a high-precision manufacturing device, demands stringent control over foundation settlement and tilting, aiming for control at the micron level. Due to the presence of cap structures, the load-bearing effect of pile groups is more rational than that of single piles. However, the interaction among caps, piles, and soil makes the settlement outcome and load transfer more complex. This article analyzes the difference in support effects between concrete and steel pipe piles in the foundation of such equipment using FLAC3D software, providing a reference for similar engineering practices.

## 2 Numerical Model Construction for the Foundation of Specific Equipment

### 2.1 Introduction to the Equipment Foundation

The foundation of the specified equipment has external dimensions of approximately  $14.1 \times 13.6$  meters, with an overall convex shape. A raft foundation approach is employed, with the main load-bearing sections having thicknesses of about 1400 mm and 1660 mm. The bearing stratum is composed of silty clay, boasting a bearing capacity of  $150 \text{ KN/m}^2$ . The parameters of various strata are as delineated in Table 1. In alignment with the weight and operational characteristics of the equipment, the permissible settlement deformation at the foundation's monitoring points is defined as 0.04 mm, and the inclination is not to exceed 0.018/1000. The site is relatively flat, previously agricultural land, with elevations ranging between 130.2 and 131.5 meters. The geomorphological unit of the investigation site is part of the high floodplain formed by the Songhua River's alluviation. The genesis of the strata includes Quaternary alluvial and siltation processes, resulting in cohesive and sandy soils. The explored strata range from top to bottom includes fill soil, cohesive soil, silty mud soil, silty sand, and medium sand.

### 2.2 Numerical Model Construction

The foundation was modeled using Rhino 6 software, through which a mesh was delineated and subsequently imported into FLAC3D software for parameter assignment and computation. The numerical model encompasses three components: piles, soil, and the cap. Piles are 24 meters in length with a side length of 0.2 meters. The elevation of the cap's base is set at -0.5 meters with a height of 1.4 meters. The soil profile consists of medium sand, silty sand, silty mud soil, cohesive soil, and fill, from bottom to top. The dimensions of the soil body are defined as 60 meters in length, 60 meters in width, and 30 meters in height, with physical parameters detailed in Table 1. Models were established for scenarios without pile support, with concrete pile support, considering friction between concrete piles and soil, and with steel pipe pile support. The calculation model is illustrated in Figure 1, and the positions of the piles are shown in Figure 2.

### 2.3 Calculation Procedure

The simulation and calculation procedure using FLAC3D software is delineated as follows:

- (1) The initial stress is considered to be the self-weight stress.
- (2) A load of 60 kPa is applied on the cap to simulate the preloading process through surcharge.
- (3) The solution is sought.
- (4) The applied load and the existing displacements are removed.
- (5) A load of 168 kPa is applied in the central area of Cap 1 to simulate the equipment load.
- (6) The final results are computed.

**Table 1.** Physical parameters of the model

| Group          | Friction Coefficient | Cohesion (MPa)   | Young's Modulus (GPa) | Density ( $\text{kg}^* \text{m}^{-3}$ ) | Poisson's Ratio | Depth (m) |
|----------------|----------------------|------------------|-----------------------|---|-----------------|-----------|
| Top1           | 61.8                 | 3.9              | 30                    | 2500                                    | 0.2             | -0.5      |
| Top2           | 61.8                 | 3.9              | 30                    | 2500                                    | 0.2             | -0.5      |
| Top3           | 61.8                 | 3.9              | 30                    | 2500                                    | 0.2             | -0.5      |
| Fill           | 15                   | 23               | $10\text{e}^{-3}$     | 2000                                    | 0.35            | -2.5      |
| Cohesive soil  | 15                   | 23               | $10\text{e}^{-3}$     | 2000                                    | 0.35            | -11.6     |
| Silty mud soil | 36                   | 0                | $28\text{e}^{-3}$     | 2000                                    | 0.35            | -13.8     |
| Silty sand     | 22                   | 46               | $5\text{e}^{-3}$      | 2000                                    | 0.35            | -21.5     |
| Medium sand    | 38                   | $5\text{e}^{-6}$ | $40\text{e}^{-3}$     | 1950                                    | 0.35            | -30       |
| Piles          | 61.8                 | 3.9              | 30                    | 2500                                    | 0.2             | -24       |

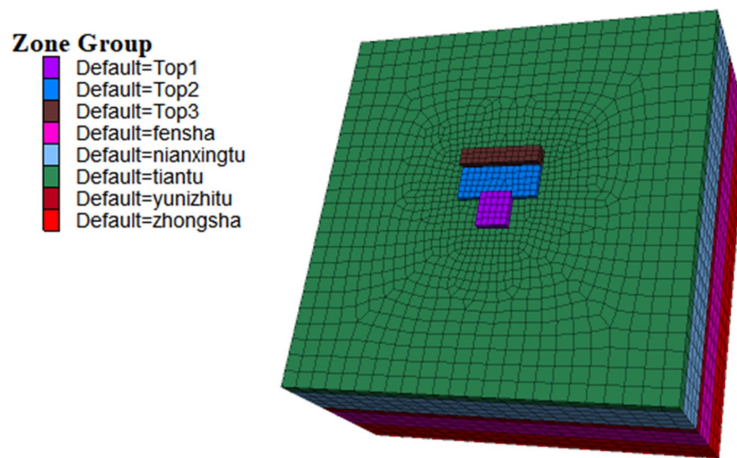


**Figure 1.** Calculation model

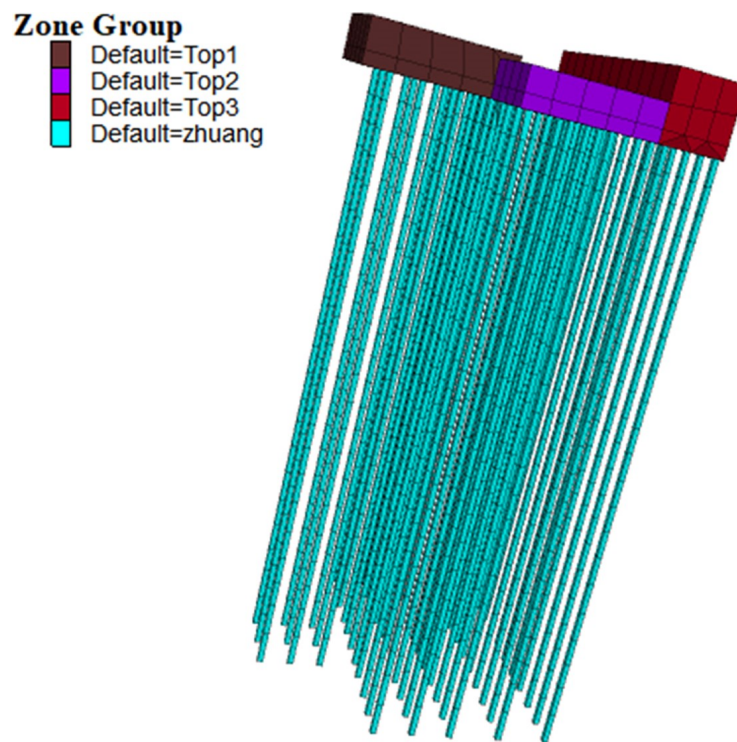


**Figure 2.** Positions of the piles

### 3 Analysis of Calculation Results

#### 3.1 Stress Analysis

Under conditions without pile support, the maximum vertical stress within the soil was observed to be 0.57 MPa. It was noted that the vertical stress within the soil increases progressively with depth. The distribution of vertical stress is illustrated in Figure 3.

With concrete pile support, an increase in vertical stress within the soil with depth was similarly observed, alongside stress concentration phenomena occurring near the pile locations. The maximum stress endured by the soil was recorded at 0.85 MPa, as depicted in Figure 4. The external load is transmitted through the cap to the concrete piles. Given the considerably greater stiffness of concrete piles compared to that of the soil, stress concentration around the piles was induced. The maximum stress on the concrete piles was found to be 7.28 MPa, as shown in Figure 5. The concrete piles functioned akin to bridges, with vertical stress being transmitted from the cap to the top of the concrete piles, subsequently propagated downwards along the piles, eventually dispersing the load borne by the cap into the deeper soil layers.

Following the consideration of the joint action between concrete piles and soil, the frictional force between pile and soil increased the resistance to interaction between the soil and the pile bodies, leading to a further increase in the vertical stress at the base of the soil around the pile bodies. Moreover, the friction-induced stress concentration between the pile bodies and the soil became more pronounced, with the maximum stress endured by the concrete piles reaching 43.3 MPa. The stress distribution in the pile bodies, taking into account the pile-soil interaction, is depicted in Figure 6.

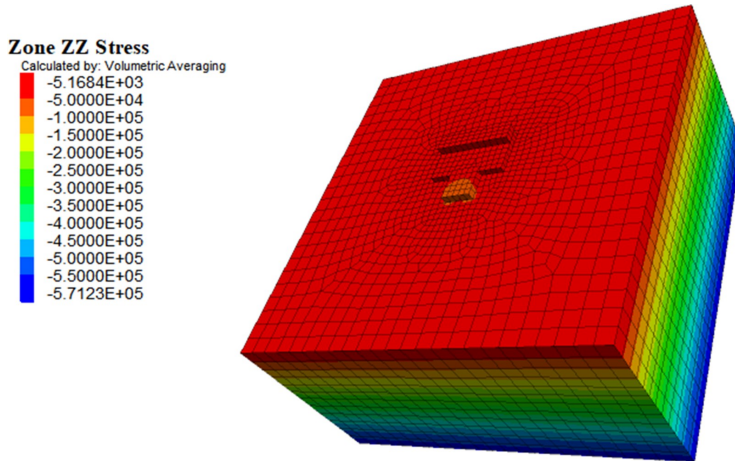


**Figure 3.** Stress distribution in the cap without piles

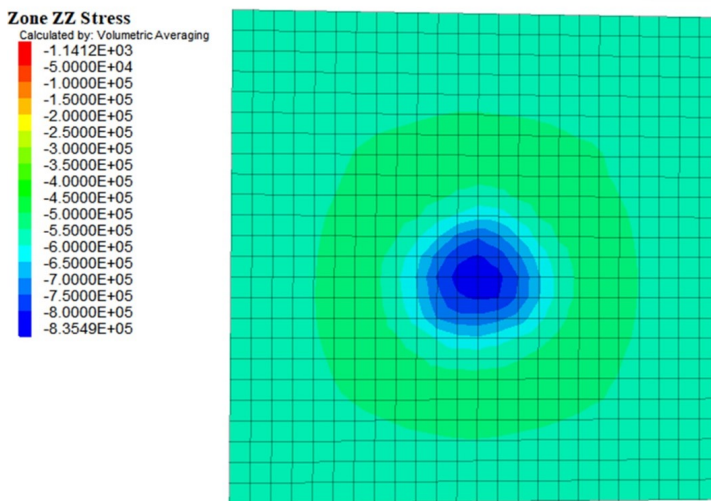


**Figure 4.** Stress distribution in soil around concrete piles

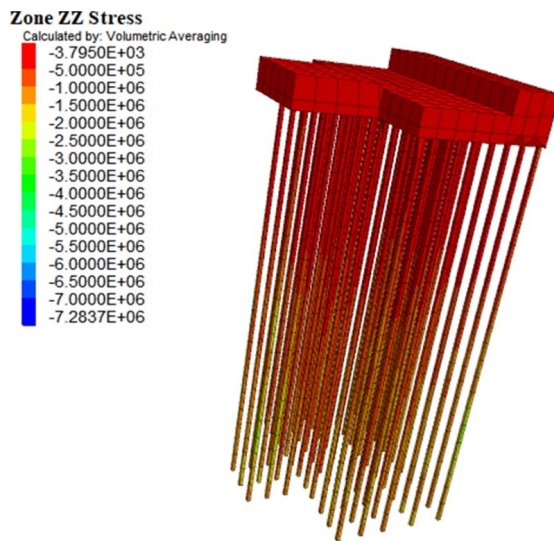


**Figure 5.** Stress distribution in concrete piles

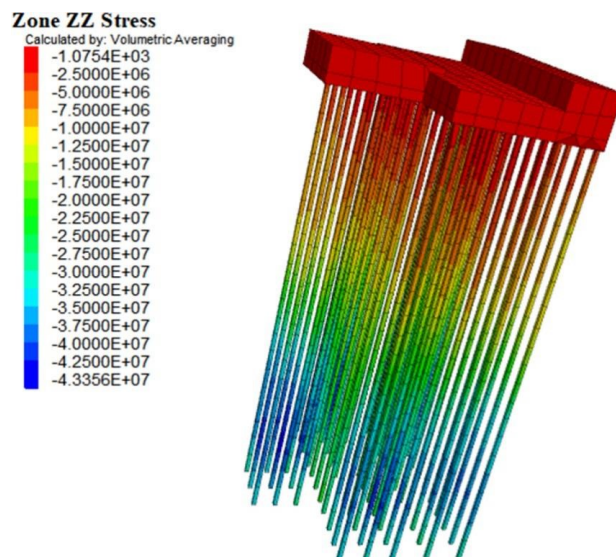


**Figure 6.** Stress distribution in pile bodies considering friction

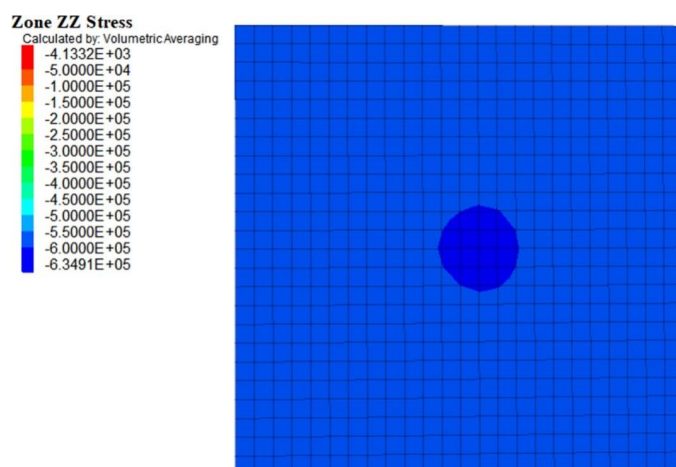


**Figure 7.** Stress distribution in the soil around steel pipe piles

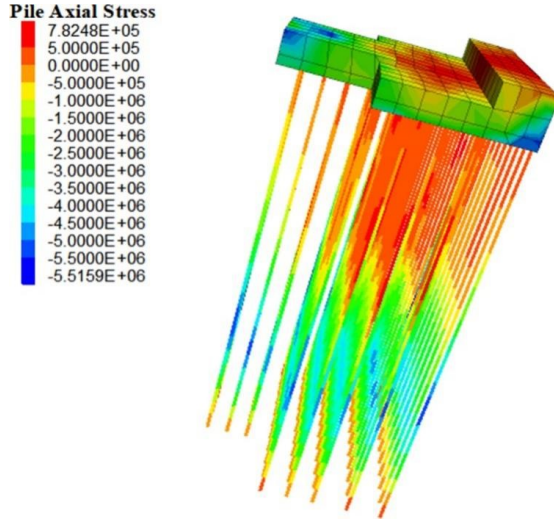


**Figure 8.** Stress distribution in steel pipe pile bodies

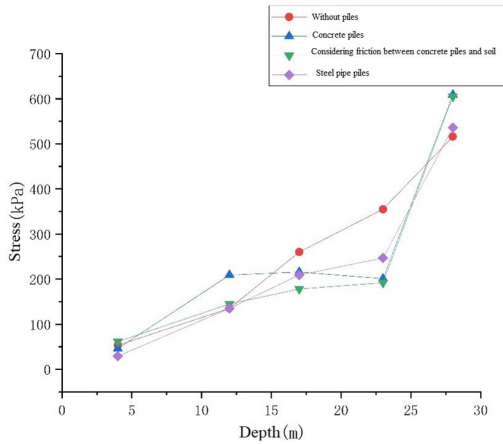


**Figure 9.** Stress distribution in different soil layers

Upon substituting concrete piles with steel pipe piles, the phenomenon of stress concentration in the soil surrounding the steel pipe piles became more significant. The stress distribution condition in the soil is shown in Figure 7, and the stress distribution in the steel pipe pile bodies is illustrated in Figure 8. The maximum stress borne by the steel pipe piles was measured at 5.52 MPa, and the maximum stress endured by the soil around the steel pipe piles was 0.63 MPa. The stress in the soil surrounding the steel pipe piles was less than that surrounding the concrete piles. The stiffness and strength of steel pipe piles exceed those of concrete piles, making steel pipe piles less prone to deformation under the same load conditions. Consequently, under external load conditions, steel pipe piles are able to more effectively share the load, leading to reduced stress in the soil. Due to the greater stiffness of steel pipe piles, the deformation they undergo when bearing loads is typically relatively smaller. Such smaller deformations may result in reduced soil displacement, diminishing the stress borne by the soil. The load is transmitted from the cap to the pile body, generating significant stress in the pile shaft, and as the load is propagated downward through the pile body, stress concentration occurs at the base of the soil.

Stress monitoring points were established at various positions around the pile bodies within different soil layers, yielding stress data for different soil layers under various support conditions, as shown in Figure 9. Under conditions without pile support, the stress within the soil increased continuously with depth. The stress in the fill layer was 53.4 kPa, in the cohesive soil layer it was 135 kPa, in the silty mud soil layer it was 260 kPa, in the silty sand layer it was 355 kPa, and in the medium sand layer it was 516 kPa. Under the condition of concrete pile support, the stress in the fill layer was 45.9 kPa, in the cohesive soil layer it was 209 kPa, in the silty mud soil layer it was 216 kPa, in the silty sand layer it was 201 kPa, and the stress in the medium sand layer increased to 609 kPa. Under steel pipe pile support conditions, the stress in the fill layer was 29.1 kPa, in the cohesive soil layer it was 135 kPa, in the silty mud soil layer it was 209 kPa, in the silty sand layer it was 247 kPa, and in the medium sand layer it was 536 kPa.

### 3.2 Analysis of Plastic Zones

A comparative analysis of the distribution of plastic zones within the soil under different support conditions is illustrated in Figure 10, Figure 11, Figure 12 and Figure 13.

Under conditions without pile support, a large extent of the soil exhibited plastic deformation. The introduction of concrete piles significantly reduced the range of the plastic zone within the soil. Concrete piles enhanced the support and constraint of the soil, thereby reducing the overall deformation of the soil, which in turn led to a reduction in the extent of the plastic zone. With the consideration of pile-soil interaction, the friction between the pile and soil increased the constraint between the soil and pile bodies, limiting soil deformation and further reducing the plastic zone. Following the implementation of steel pipe piles, due to their higher rigidity and load-bearing capacity, an even more effective limitation on the overall deformation of the soil was observed, resulting in a further reduction in the extent of the plastic zone.

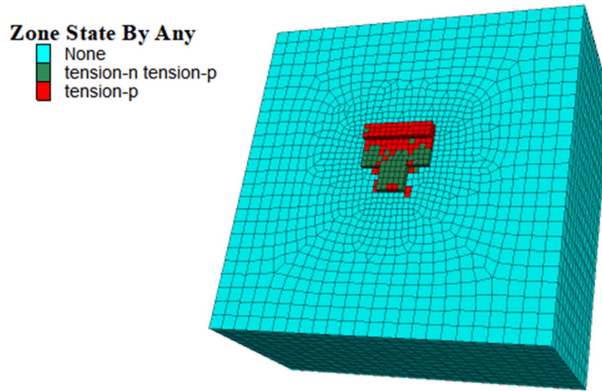


**Figure 10.** Plastic zone without piles

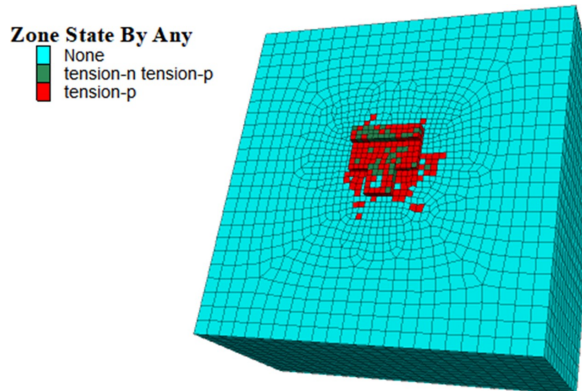


**Figure 11.** Plastic zone with concrete piles

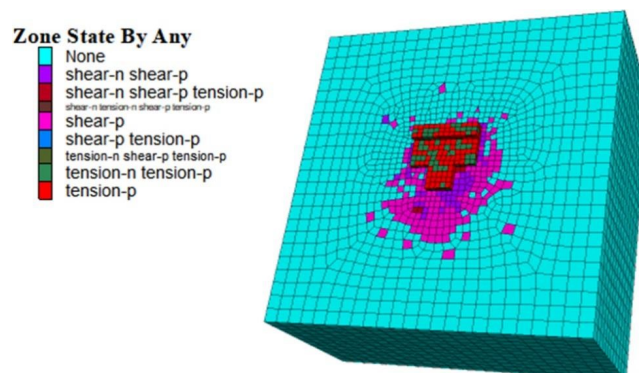


**Figure 12.** Plastic zone considering friction

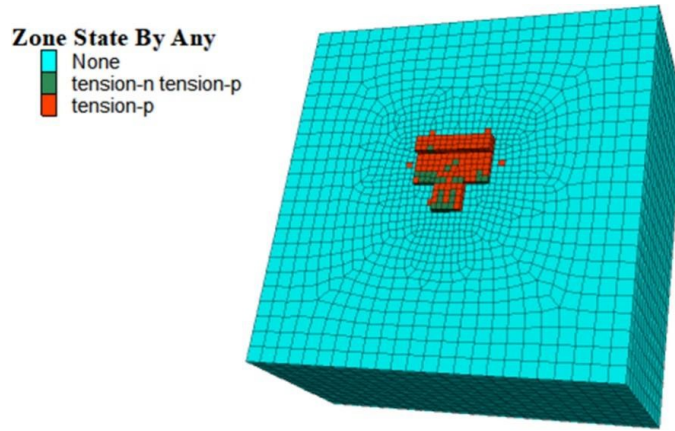


**Figure 13.** Plastic zone with steel pipe piles

### 3.3 Settlement Analysis

The settlement results for the soil under conditions without pile support are illustrated in Figure 14, while the settlement results under concrete pile support conditions are shown in Figure 15. The settlement outcomes considering the combined action of concrete piles and soil are depicted in Figure 16. Following the implementation of concrete piles, the maximum settlement of the soil decreased from 15.78 mm to 4.12 mm. Considering the combined action of concrete piles and soil, the maximum settlement further reduced to 3.91 mm. The settlement results after substituting concrete piles with steel pipe piles are presented in Figure 17, where the use of steel pipe piles reduced the minimum soil settlement to 2.38 mm.

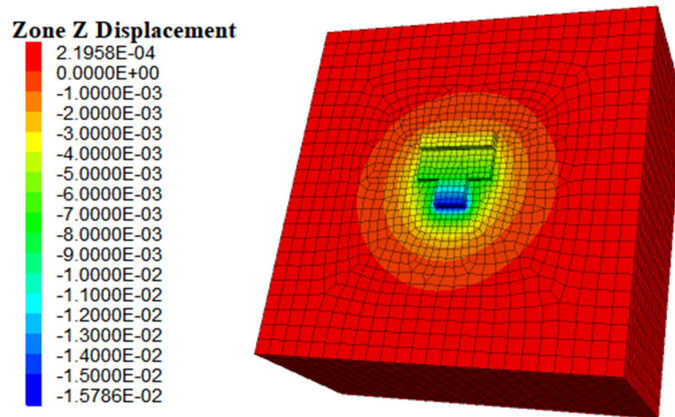


**Figure 14.** Settlement results without piles

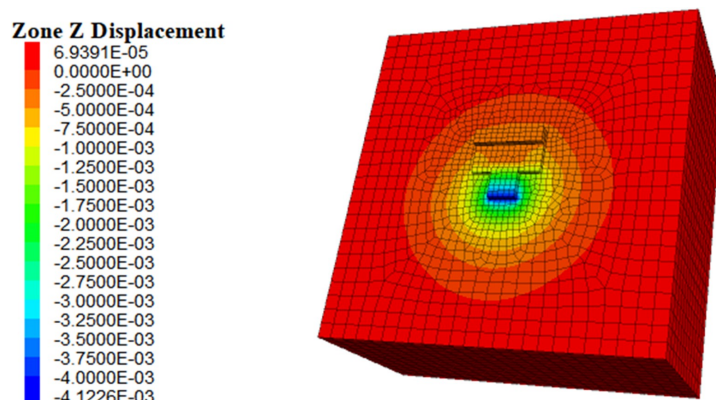


**Figure 15.** Settlement results with concrete piles

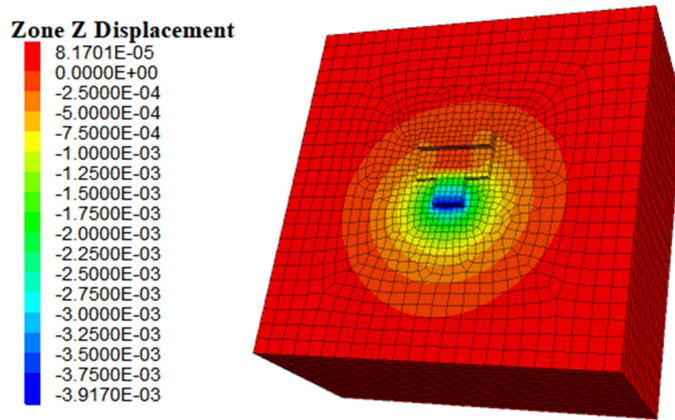


**Figure 16.** Settlement considering friction between concrete piles and soil

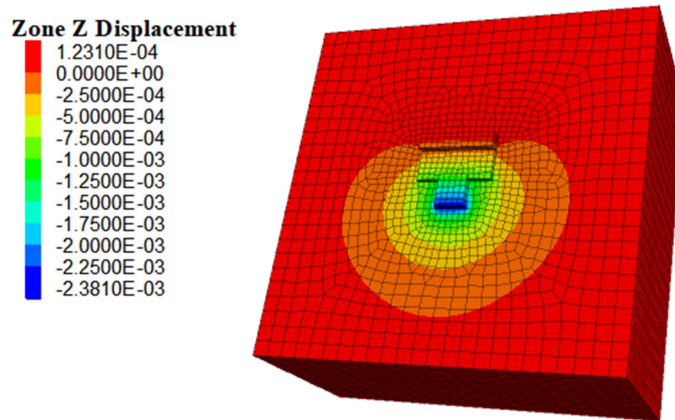


**Figure 17.** Settlement results with steel pipe piles

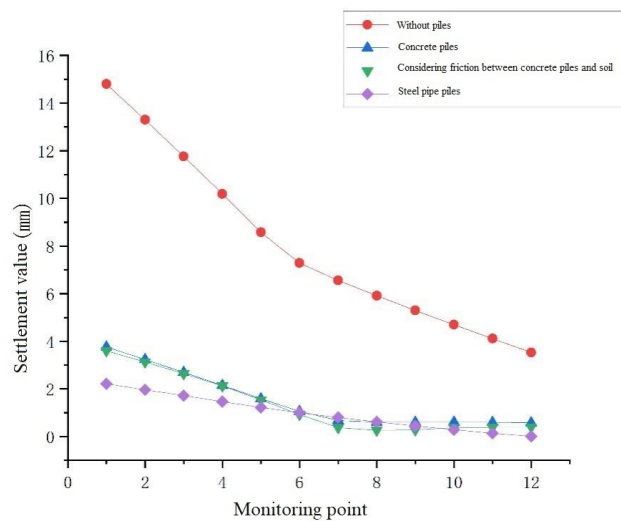


**Figure 18.** Settlement of different support models

Twelve monitoring points were established beneath the cap to observe the settlement under different support models, with the settlement values depicted in Figure 18. Under conditions without pile support, significant settlement occurred within the soil, with the maximum settlement recorded at 14.80 mm and the minimum at 3.53 mm, resulting in a differential settlement of 11.27 mm. Following the implementation of concrete piles, a notable reduction in soil settlement was observed, with the maximum settlement reducing to 3.77 mm, the minimum to

0.58 mm, and the differential settlement to 3.19 mm. Considering the combined action of concrete piles and soil, soil settlement further decreased, with the maximum settlement at 3.59 mm, the minimum at 0.40 mm, and the differential settlement remaining at 3.19 mm. The friction between pile and soil increased the resistance of their interaction, mitigating the overall deformation tendency of the foundation. Substituting concrete piles with steel pipe piles resulted in a maximum settlement of 2.21 mm, a minimum settlement of 0.02 mm, and a differential settlement of 2.19 mm. The settlement values and differential settlement with steel pipe piles were significantly reduced compared to those with concrete piles, indicating that steel pipe pile support not only effectively reduces settlement but also better controls differential settlement.

#### 4 Conclusions

(a) Under conditions with only a cap in place, significant soil settlement was observed, with the maximum reaching 15.78 mm and a differential settlement of 11.27 mm. Soil stress was found to increase progressively with depth, reaching a maximum of 0.57 MPa, and a considerable extent of the soil exhibited plastic deformation.

(b) The application of concrete piles resulted in a reduction of soil settlement to 4.12 mm, with pile settlement recorded at 3.47 mm, and a differential settlement of 3.19 mm. Stress concentration phenomena occurred in the soil adjacent to the piles, with the maximum soil stress increasing to 0.84 MPa, and pile stress reaching 7.28 MPa. Considering the combined action of concrete piles and soil, soil settlement further decreased to 2.59 mm, with pile settlement at 2.23 mm, and the differential settlement remaining at 3.19 mm. The stress on concrete piles increased to 43.3 MPa.

(c) Substituting concrete piles with steel pipe piles led to a maximum soil settlement of 2.38 mm, pile settlement of 1.22 mm, and a differential settlement of 2.19 mm. The phenomenon of stress concentration in the soil surrounding steel pipe piles became more pronounced, with soil stress near steel pipe piles at 0.63 MPa, and the stress on steel pipe piles at 5.52 MPa. Steel pipe piles were more effective than concrete piles in reducing soil settlement.

#### Data Availability

The data used to support the research findings are available from the corresponding author upon request.

#### Conflicts of Interest

The authors declare no conflict of interest.

#### References

- [1] J. L. Liu and L. Q. Chi, “The modified model of pile-soil deformation calculation and variable rigidity design method for balance settlement,” *Chin. J. Geotech. Eng.*, vol. 22, no. 2, pp. 151–157, 2000.
- [2] L. Q. Guo, M. Liang, and F. Q. Chen, “Finite element analysis on soil-pile interaction behavior subjected to repeated surcharge load,” *J. Huaqiao Univ. (Nat. Sci.)*, vol. 32, no. 5, pp. 569–578, 2011. <https://doi.org/10.1830/ISSN.1000-5013.2011.05.0569>
- [3] F. Hu, “Study on pile-soil interaction of soft soil area in Putian city, Fujian province,” *Geol. Fujian*, vol. 40, no. 1, pp. 66–76, 2021.
- [4] G. Q. Kong, Q. Yang, P. Y. Zheng, and M. T. Luan, “Model tests on negative skin friction for pile groups considering time effect,” *Chin. J. Geotech. Eng.*, vol. 31, no. 12, pp. 1913–1919, 2009.
- [5] R. D. Qiu, J. L. Liu, W. S. Gao, and M. B. Qiu, “Some problems on settlement calculation of pile group foundation,” *Chin. J. Geotech. Eng.*, vol. 33, no. S2, pp. 15–23, 2011.
- [6] Y. B. Mao, G. L. Dai, and W. M. Gong, “Settlement of pile groups based on static load tests on single pile,” *Chin. J. Geotech. Eng.*, vol. 35, no. zk2, pp. 627–631, 2013.
- [7] C. J. Zheng, Y. Q. Cui, X. M. Ding, and L. B. Luan, “Analytical solution for dynamic interaction of end-bearing pile groups subjected to vertical dynamic loads,” *Chin. J. Geotech. Eng.*, vol. 44, no. 12, pp. 2187–2195, 2022. <https://doi.org/10.11779/CJGE202212005>
- [8] S. Zhang, C. Cui, and G. Yang, “Vertical dynamic impedance of pile groups partially embedded in multilayered, transversely isotropic, saturated soils,” *Soil Dyn. Earthq. Eng.*, vol. 117, pp. 106–115, 2019.
- [9] X. Ding, L. Luan, C. Zheng *et al.*, “Influence of the secondorder effect of axial load on lateral dynamic response of a pipe pile in saturated soil layer,” *Soil Dyn. Earthq. Eng.*, vol. 103, pp. 86–94, 2017.
- [10] Z. Y. Ai, C. L. Liu, L. J. Wang *et al.*, “Vertical vibration of a partially embedded pile group in transversely isotropic soils,” *Comput. Geotech.*, vol. 80, pp. 107–114, 2016.
- [11] S. P. Zhang, C. Y. Cui, and G. Yang, “Vertical dynamic impedance of pile groups partially embedded in multilayered, transversely isotropic, saturated soils,” *Soil Dyn. Earthq. Eng.*, vol. 117, pp. 106–115, 2019.

- [12] L. Luan, C. Zheng, G. Kouretzis, G. Cao, and H. Zhou, “Development of a three-dimensional soil model for the dynamic analysis of end-bearing pile groups subjected to vertical loads,” *Int. J. Numer. Anal. Methods Geomech.*, vol. 43, no. 9, pp. 1784–1793, 2019. <https://doi.org/10.1002/nag.2932>
- [13] B. B. Sheil, B. A. McCabe, E. M. Comodromos *et al.*, “Pile groups under axial loading: An appraisal of simplified non-linear prediction models,” *Geotechnique*, vol. 69, no. 7, pp. 565–579, 2019.
- [14] H. Zhou, H. Liu, M. F. Randolph, G. Kong, and Z. Cao, “Experimental and analytical study of X-section cast-in-place concrete pile installation effect,” *Int. J. Phys. Model. Geotechnics*, vol. 17, no. 2, pp. 103–121, 2017.
- [15] C. Zheng, X. Ding, and Y. Sun, “Vertical vibration of a pipe pile in viscoelastic soil considering the three-dimensional wave effect of soil,” *Int. J. Geomech.*, vol. 16, no. 1, p. 04015037, 2015. [https://doi.org/10.1061/\(ASCE\)GM.1943-5622.0000521](https://doi.org/10.1061/(ASCE)GM.1943-5622.0000521)
- [16] G. Anoyatis, G. Mylonakis, and A. Lemnitzer, “Soil reaction to lateral harmonic pile motion,” *Soil. Dyn. Earthq. Eng.*, vol. 87, pp. 164–179, 2016. <https://doi.org/10.1016/j.soildyn.2016.05.023>
- [17] M. F. Torshizi, M. Saitoh, G. M. Álamo *et al.*, “Influence of pile radius on the pile head kinematic bending strains of end-bearing pile groups,” *Soil. Dyn. Earthq. Eng.*, vol. 105, pp. 184–203, 2018. <https://doi.org/10.1016/j.soildyn.2017.11.040>
- [18] Z. Y. Ai, P. C. Li, B. K. Shi *et al.*, “Influence of a point sink on a pile group in saturated multilayered soils with anisotropic permeability,” *Int. J. Numer. Anal. Methods Geomech.*, 2018. <https://doi.org/10.1002/nag.2769>
- [19] C. Cui, K. Meng, Y. Wu *et al.*, “Dynamic response of pipe pile embedded in layered visco-elastic media with radial inhomogeneity under vertical excitation,” *Geomech. Eng.*, vol. 16, no. 6, pp. 609–618, 2018. <https://doi.org/10.12989/gae.2018.16.6.609>
- [20] L. A. Padrón, J. J. Aznárez, and O. Maeso, “BEM–FEM coupling model for the dynamic analysis of piles and pile groups,” *Eng. Anal. Bound. Elem.*, vol. 31, no. 6, pp. 473–484, 2007. <https://doi.org/10.1016/j.enganabound.2007.01.008>